applied sciences

MDPI

Review

Making a Case for Hybrid GFRP-Steel Reinforcement System in Concrete Beams: An Overview

Rajeev Devaraj *, Ayodele Olofinjana and Christophe Gerber

School of Science, Technology and Engineering, University of the Sunshine Coast, 90 Sippy Downs Dr, Sippy Downs, QLD 4556, Australia
* Correspondence: rajeev.devaraj@research.usc.edu.au

Abstract: Ageing concrete infrastructures are known to be facing deterioration, especially regarding the corrosion of their reinforcing steel. As a solution, glass fibre-reinforced plastic (GFRP) bars are now considered a reinforcement alternative to conventional steel, and design codes now exist for designing GFRP-RC structures. However, there is a need to improve on addressing the limited plastic yield in GFRPs. Consequently, it is suggested that a hybrid steel–GFRP RC system can enhance the mechanical performance of flexure beams up to the required standard and, at the same time, address the durability concerns of steel-only RC beams. This overview presents the studies conducted to enhance the performance of hybrid GFRP–steel RC beams by reviewing the analytical models proposed to improve the various aspects of reinforcement design. The models consider mechanical effects such as ductility, crack width, flexure and shear, and the physical effects such as thermal stability when exposed to the temperature. Though the evidence reviewed supports the viability of the hybrid GFRP–steel reinforcing system to address ductility, much is still required in the area of research, as highlighted in the future outlook.

Keywords: glass fibre reinforced polymer (GFRP); hybrid GFRP-steel reinforcement; concrete beams; ductility; flexural design

check for updates

Citation: Devaraj, R.; Olofinjana, A.; Gerber, C. Making a Case for Hybrid GFRP-Steel Reinforcement System in Concrete Beams: An Overview. *Appl. Sci.* **2023**, *13*, 1463. https://doi.org/10.3390/app13031463

Academic Editors: Alexey Beskopylny, Anatoly Lavrentyev, Evgenii Shcherban and Sergei Stel'makh

Received: 21 December 2022
Revised: 18 January 2023
Accepted: 18 January 2023
Published: 22 January 2023

Copyright: © 2023 by the authors. Licensee MDPI, Basel, Switzerland. This article is an open access article distributed under the terms and conditions of the Creative Commons Attribution (CC BY) license (https://creativecommons.org/licenses/by/4.0/).

1. Introduction

The durability of a reinforced concrete (RC) structure is associated with many factors [1–4], and most of them are related to the corrosion of steel reinforcement bars. This is a general problem that can affect the integrity of assets built to last for extended service life periods. Studies on the durability of steel embedded in concrete structures now generate a lot of interest, as exemplified in recent publications [5–10]. Numerous structures have been examined for their structural integrities, and corrosion is identified as a significant threat affecting these assets' durability [11–14].

Glass Fibre Reinforced Polymer (GFRP) bars as an alternative to steel reinforcement in concrete structures have been receiving increased attention over the past two decades [15–19]. Due to its inherent corrosion resistance, GFRP has gained a reputation [20–22] as an alternative to steel in RCs to meet the requirements of durability in aggressive environments. GFRP is known to exhibit high tensile strength, typically about 1100 MPa, compared to steel, generally considered to be about 400 MPa. However, GFRP is not known to exhibit the classic plastic yielding known in steel before failing. Concrete structures reinforced with GFRPs may show little evidence of overload–cracking–development and excessive deformation until beyond their ultimate limit state due to the lack of plasticity in the reinforcement elements [23–25]. The established design philosophy in RC structures relied on steel reinforcement to provide sufficient ductility to prevent concrete elements from unpredictable failure by leveraging on the elastic deformation and the plasticity of steel. On the other hand, the lower elasticity of GFRP allows for larger elastic deformation but offers no protection from brittle failure. The limited intrinsic ductility in GFRP leads to designing flexure beams with over-reinforced character and conservative safety coefficients.

Though the latest design standards, such as ACI-440.11-22 put forward methods to design GFRP-only reinforced structures, the lack of discernible plasticity in GFRP itself remains a concern on the suitability of GFRP rebars as a complete replacement for the steel rebars in concrete. The designers' reticence to specify over-reinforced structures still places steel as favourable to GFRP [26–28]. Hybrid reinforcement concepts of GFRP and steel reinforcement where steel confers ductility and GFRP provide strength is the concept being proposed [29–31] to address the possibility of brittle failures in RCs with complete replacement of steel with GFRP. In this arrangement, GFRP takes the primary reinforcement role and governs the ultimate state whilst the steel reinforcement controls the failure mode [32–38]. Furthermore, the steel bars are located more interiorly in the RC element to ensure sufficient concrete cover protection without increasing the total depth of the beam whilst sufficiently governing the required ductile failure mode.

Although the hybrid GFRP–steel RC beams have many advantages, their reinforcement arrangements must be optimal to leverage strength and ductility. Their structural behaviour also needs to be understood to achieve a safe and accurate design for construction. Thus, many investigations [39–43] have considered the various aspects of hybrid GFRP-steel RC beams and proposed different design models to identify optimal reinforcement arrangements. This paper reviews the related analytical models that assess the behaviour of hybrid beams under various mechanical and physical effects. The review outlines the challenges and the need for further research for the safe and reliable application of hybrid GFRP–steel RC beams.

2. Background

2.1. Steel Deterioration in RC Beams

Corrosion of steel reinforcement in concrete structures can lead to reduced structural integrity and service life. When steel reinforcement corrodes, it expands and can cause the concrete to crack and spall, leading to a loss of bond between the steel and concrete. This can result in reduced load-carrying capacity and increased risk of structural failure. The corrosion process of steel in concrete structures is facilitated by the presence of water and oxygen, as well as chloride ion contamination, which can come from sources such as seawater or de-icing salts. As the steel corrodes, the volume expansion accompanying the chemical products pushes on the surrounding concrete, leading to the formation of cracks and voids in the concrete cover. This can expose the steel to further corrosion, leading to a vicious cycle of deterioration.

Concrete, on its own, because of its intrinsic mechanical property, is susceptible to cracking and is also a permeable material. The combination of intrinsic porosity and cracks through capillary action provides pathways for electrolytes to reach the embedded steel reinforcement in a concrete body. In a favourable atmospheric condition, dissolved ions of chlorides (Cl^-) or carbonates (CO_3^-) provide the electrolytic potential for corrosion [44–47]. Concrete carbonation and the infiltration of chloride ions cause changes in the pore solution of concrete, present within the pores or voids in the material. Such conditions would aid the galvanic mechanism responsible for the corrosive attack on steel reinforcements, leading to significant corrosion damage. Additionally, carbonation results in acidification due to the penetration of atmospheric CO_2, and the presence of chloride ions can cause steel corrosion through pitting. Figure 1 presents the schematic illustration of the corrodent transport in RCs [48]. The diffusive travel of corrodents is resisted by the concrete cover, typically taken to be 30–50 mm. In several studies [49–54], corrosion damage has been reported to be responsible for the reductions in service life and the ultimate capability of RC structures.

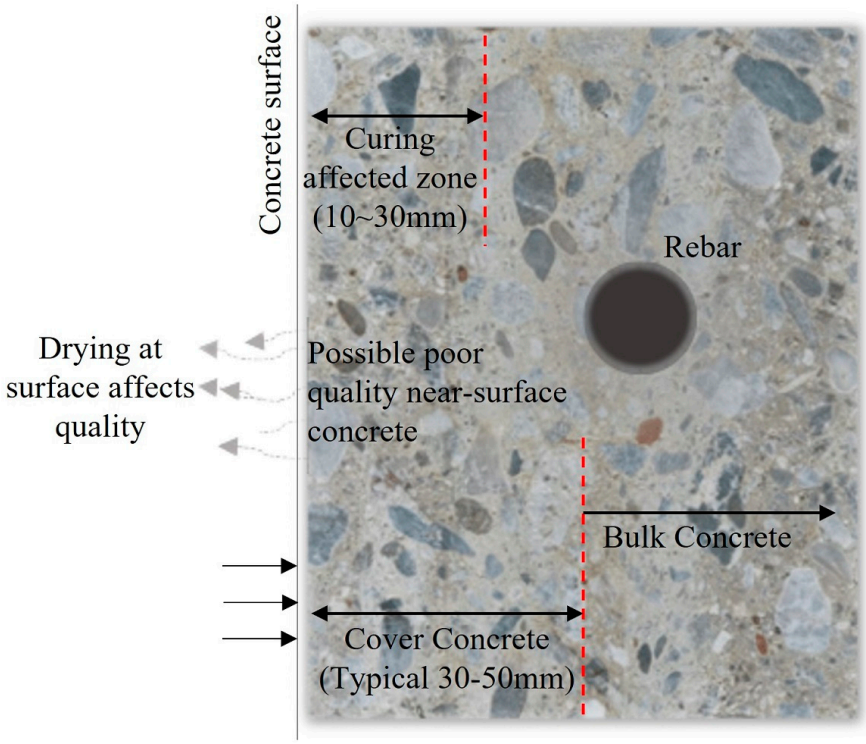


Figure 1. Schematic illustration of corrosion attack path in RC [48]. Reproduced with permission from Elsevier 2023.

2.2. Fibre Reinforced Polymers (FRP) as Alternative Reinforcement in RC Beams

The established corrosion protection methods, such as epoxy-coating, galvanic coating, and anodic protection that are currently used in the industry only act as temporary solutions and sometimes can be expensive and impractical. A more durable approach may be to use Fibre Reinforced Polymer (FRP) instead of steel. The earliest use of FRP composite materials in the construction industry dates back to the 1970s when they were used to rehabilitate a bridge girder in Japan [55]. It was followed by many rehabilitations as well as projects where FRP bars in RC structures were successfully implemented [56–58]. Several studies [59–61] are currently in progress to further the development of FRP applications in RC beams. These studies focus on advancing the utilisation of FRP for retrofitting and new build purposes.

The early use of Carbon Fibre Reinforced Polymers (CFRP) demonstrated its potential and became prevalent in the retrofitting industry [62,63]. The success fuelled the demand for CFRP, but due to the limited supply, the commercial price of CFRPs increased substantially. As a result, its use in a large volume was no longer economically feasible. The strength of carbon fibres and other engineering fibres for FRPs are shown in Figure 2. The high strength of carbon fibres as depicted in Figure 2 made it the material of choice in FRP design for structural applications, and CFRP is generally a highly valued engineering composite. However, the relatively high price of carbon fibres (Figure 2) compared to the other types of engineering fibres for FRP made CFRP too costly to be viable as a construction material. Figure 2 shows the relative costs of engineering fibres and thus indicates that CFPRs could be 10 to 30 times more expensive than GFRPs another lower-priced fibres with comparative tensile strength.

Apart from carbon fibres, alternative FRPs are made from glass- (GFRP), aramid- (AFRP), and basalt (BFRP) fibres. The composite property of FRP is inherently dependent on the intrinsic properties of the reinforcing fibres. The primary mechanical properties of strength and modulus versus density are shown in Figures 3 and 4. It is shown that Aramid (Kevlar) fibres have the best tensile strength to the density ratio and show good resistance to most types of chemicals. However, they are sensitive to humidity and UV light and

degrade when exposed to several acids and alkalis [64]. Their highly variable value of Young's modulus (Figure 4) made it not suitable for FRP in construction materials. Basalt fibres, manufactured by melting weathered volcanic lava, are characterised by high strength and high values of Young's modulus and have the highest thermal resistance amongst the engineering fibres, with a melting temperature of 1450 °C. On the other hand, basalt fibres are more vulnerable to alkaline effects and are rarely used in practical engineering FRPs [65].

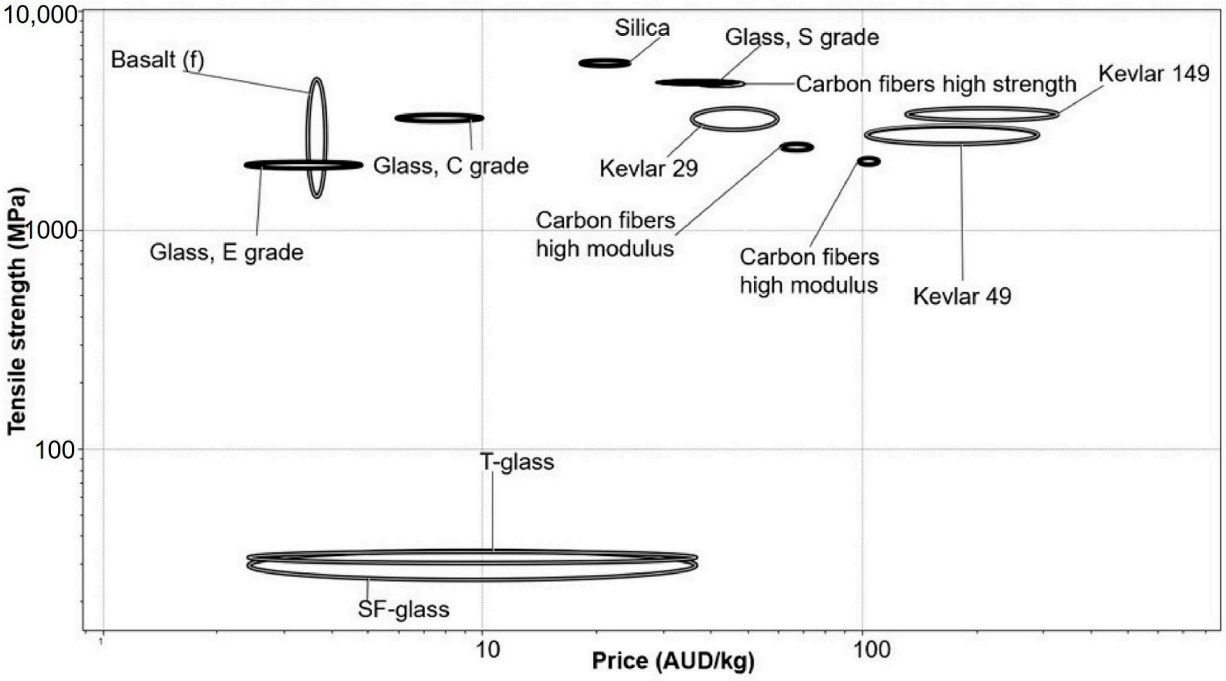


Figure 2. Tensile Strength versus Price (Generated by CES EduPack, 2015).

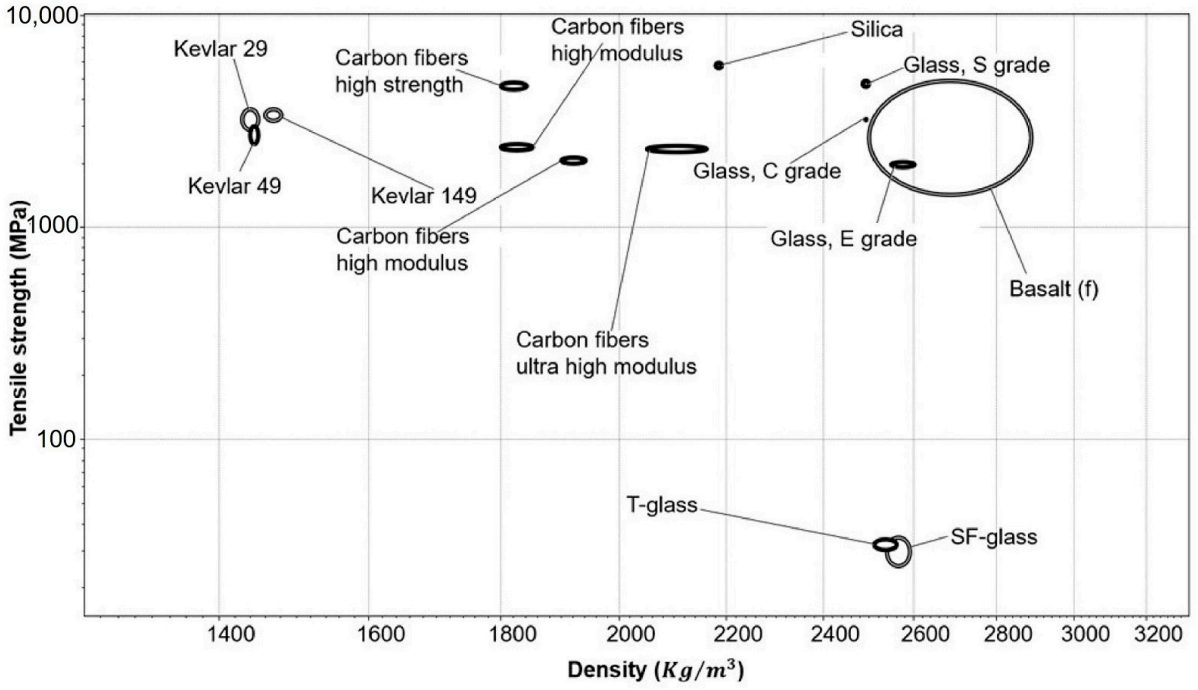


Figure 3. Tensile strength versus density (Generated by CES EduPack, 2015).

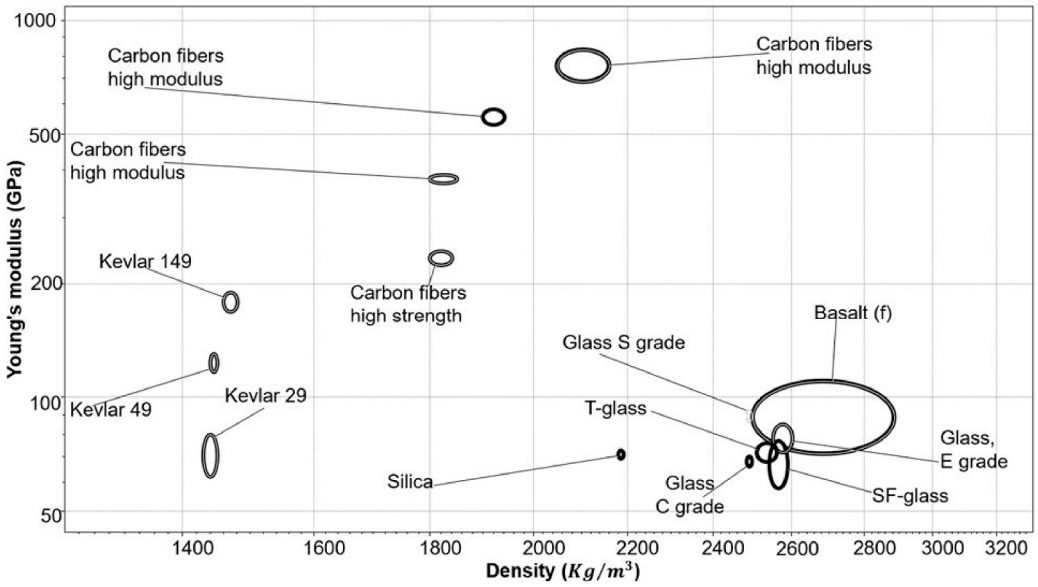


Figure 4. Young's Modulus vs. Density (Generated by CES EduPack, 2015).

Glass fibres with high strength and modest Young's modulus are the most commonly used fibres for commercial construction amongst the FRP family. They can be produced cheaply and are applicable in engineering applications where the high stiffness of carbon fibres is not required [66]. Therefore, applying GFRP bars in construction is the most economically feasible. It is now receiving more attention as it represents a viable alternative to steel reinforcement in order to address corrosion-related durability issues in conventional concrete structures [67].

Table 1 gives an overview of the market's performance and appraisal of the commercially available FRPs (GFRP, CFRP and BFRP) variants.

Several studies [68–72] have been conducted to study the durability of GFRP bars in harsh conditions. It is generally observed that the durability mechanism of GFRP is largely based on resin hydrolysis, fibre degradation, and interfacial bonding behaviour after exposure to hygrothermal conditions and fatigue regimes. This clearly highlight the importance of materials design for GFRP to using materials that can withstand such environmental degradative actions by choice and design of resin mixes. Other works [68–71] suggested that using nano-composite and E-glasses advantages the durability of GFRP in harsh environments. Additionally, some studies [72,73] recommended carbon/glass fibre-reinforced polymer hybrid (HFRP) in critical applications such as oil wells and bridges to address these durability issues. However, while there may be concerns about the limitations of GFRPs on their long-term durability, there are pieces of evidence presented [74–76] that has highlighted GFRP advantages over steel rebars in tackling durability concerns in RC structures.

Though GFRP only shows half the compression strength of steel, it is not a disadvantage since reinforcements are meant to take tensile loads, and for that reason, its functionality as a reinforcing element is enabled by its proven tensile strength [77]. However, to achieve similar elastic-plastic behaviour of steel RC systems, some studies [78–80] experimented with combinations of different types of FRP reinforcements. Although such combinations gave good results in laboratory tests and in computer simulations, the high initial cost restricts the use of non-GFRP composites in commercial applications [81].

The ratio of post-yield deformation to yield deformation characteristics favours the steel to govern the ductility in RC structures [82]. A series of investigations have identified that ductile response of steel can effectively be initiated in concrete beams with hybrid GFRP–steel reinforcements [83–87], therefore achieving enhanced ductility compared to GFRP-only RC beams. Current design standards, such as those of the American Concrete Institute [88] allow hybrid GFRP-steel solutions in large-scale concrete works. Though there

is convincing evidence on the workability of hybrid GFRP–steel RCs, the research works are moderately limited. There is still a need to understand more about their structural response and how they could be optimised. This paper reviews the literature on hybrid GFRP–steel reinforcement systems and provides an outlook for future research.

Table 1. Overview of FRP variants.

	Tensile Strength (MPa)	Compressive Strength (MPa)	Young's Modulus (GPa)	Advantages	Disadvantages
GFRP	600–1100	100–400	45–80	- High tensile strength compared to steel reinforcement - Corrosion resistance - Can be easily cut and shape - Low cost - Can be used in wet and dry conditions - Non-conductive	-Lower strength compared to CFRP and BFRP
CFRP	1500–4000	600–200	120–400	-Very high tensile strength -High strength-to-weight ratio -Corrosion resistant -Good fatigue resistance -Non-conductive	-Higher cost compared to GFRP
BFRP	1000–3000	400–1500	70–200	-High tensile strength -High strength-to-weight ratio -Corrosion resistant -Non-conductive	-Lower availability and higher cost compared to GFRP -Potential for delamination

3. Analytical Models for Hybrid GFRP-Steel Reinforced Beams

3.1. Models Considering Mechanical Effects

3.1.1. Ductility Analysis

Ductility refers to the ability of a material to endure loads whilst experiencing significant strain before failure. Figure 5 compares the idealised ductile behaviour of GFRP and steel reinforcements [89]. Ductile responses are a significant aspect of the performance of GFRP-steel hybrid beams [90,91], where the implementation of hybrid concepts aims to achieve enhanced ductility of flexural beams [92,93].

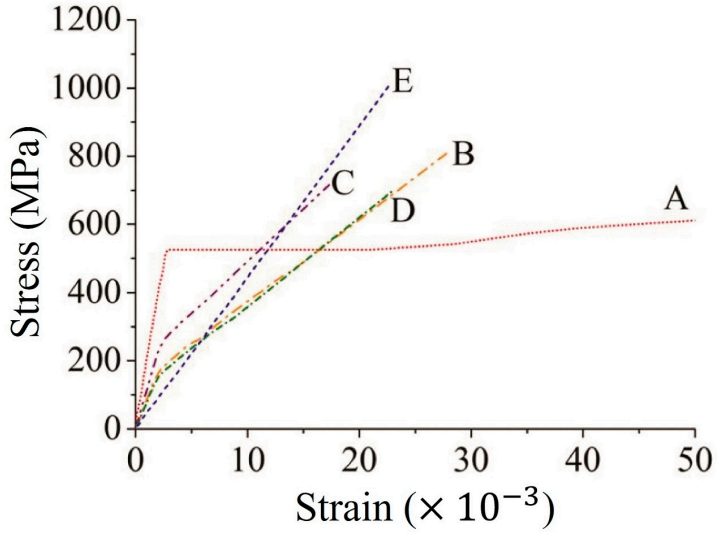


Figure 5. Tensile behaviour of steel compared to FRP (A) Steel, (B) Basalt FRP, (C) Basalt FRP, (D) Glass FRP, (E) Basalt FRP [89]. Reproduced with permission from Springer Nature 2023.

The objectives of the studies conducted in this area are framed to provide evidence that the hybrid application of steel and GFRP can significantly improve their ductility performance compared to the GFRP-only reinforcement [94,95]. Such outcomes led to further investigations on the requirement for ductility models applicable to make the hybrid reinforcement design safer and more efficient. However, conventional ductility concepts cannot be suitably applied to hybrid systems without modifications [96]. Traditional ductility models are described on the foundational concepts of cracking, yielding, and ultimate points. The current ductility indices are derived from stress–strain information of steel between yielding and ultimate stress where there is significant plastic deformation. For GFRP RC, the ductility indices become complex since the stiffness of GFRPs is considerably lower than that of steel and also because it does not exhibit the characteristic yielding at ultimate stress that is accompanied by large plasticity as the case in steel.

Conventional ductility indices and concepts are arguably not valid for beams with GFRP reinforcements [91,97–99]. Though design codes now exist for designing GFRP RCs, there is a need to develop a more reliable design approach that would consider the complexity of defining the ductility of hybrid GFRP-Steel RCs [100].

Different parameters related to deformation are generally used to express the ductility indices, include displacements, curvatures, and rotations. However, such approaches are unsuitable for GFRPs as they do not incorporate indices related to the primary characteristics and behaviour of GFRPs. New parameters are proposed to quantify the ductility of concrete beams reinforced with hybrid GFRP-steel bars [99]. Two major approaches are considered in developing updated equations [101,102]:

deformation-based, which relies on equivalent deformability factor μ_M, and

energy-based where the factor μ_{en} defines the ductility as energy absorbing capacity.

Based on these concepts, these approaches were considered in the development of analytical models that express the ductility of hybrid GFRP–steel reinforced concrete beams.

Taking the energy approach, Grace et al. [97] propose Equation (1) that expresses ductility as the ratio of the total energy to the elastic energy at the failure state of a beam. This approach utilises the elastic energy (E_{ela}) prior to failure. The total energy (E_{tot}) is taken as the area under the moment–curvature or load–deflection curve and E_{ela} as the elastic energy. The ductility index μ_{en} was expressed as [97]:

$$\mu_{en} = 0.5\left(\frac{E_{tot}}{E_{ela}} + 1\right) \tag{1}$$

A new term "deformability" has been defined in Equation (2) [103]. It is intended to be used as a replacement of the conventional term ductility in design equations. This approach proposes an equivalent deformability factor as the ratio of the beam's equivalent deformation (Δ_t) of the uncracked section to the actual deformation (Δ_u) observed at the ultimate state of the section. This model gives a μ value that is three times larger than the value given by the conventional ductility index:

$$\mu = \frac{\Delta_u}{\Delta_t} \tag{2}$$

A different approach to defining ductility in GFRP-RCs includes the consideration of strains at curvature. This model, proposed by Mufti et al. [104] was developed based on the failure of concrete crushing. As shown in Equation (3), it is an expression of the product of the ratio of curvature at ultimate state to the curvature when a strain of 0.001 is exhibited at the extreme compression edge of the RC section, i.e., ε_c = 0.001, and the ratio of the ultimate moment to that of the corresponding moment at ε_c = 0.001.

$$\mu_m = \left(\frac{\varphi_u}{\varphi_{0.001}}\right)\left(\frac{M_u}{M_{0.001}}\right) \tag{3}$$

where φ_u is the curvature at ultimate state; $\varphi_{0.001}$ corresponds to the curvature when $\varepsilon_c = 0.001$; M_u is the ultimate moment; and $M_{0.001}$ corresponds to the moment at $\varepsilon_c = 0.001$.

A comprehensive performance factor J, combining deformability and strength, can be defined by the ratio of two energy quantities associated with the ultimate limit state condition and the proportional limit of the extreme compression zone [105] of the RC section. J must be a minimum of 4.0 for rectangular sections and at least 6.0 for T-sections, noting these design criteria have been included in the Canadian Highway Bridge Design Codes [106]. The J-factor is expressed as [105]:

$$J = \left(\frac{M_{ult} \Psi_{ult}}{M_c \Psi_c} \right) \tag{4}$$

where M_{ult} expresses the ultimate moment capacity of the section; M_c is the moment at $\varepsilon_c = 0.001$; Ψ_{ult} is the curvature at M_{ult} and Ψ_c is the curvature at M_c.

The overall deformability factor Z considers the cracking behaviour in the ductility model. As expressed in Equation (5) [99], the effect of cracking is accounted for with the ratios of deflections at ultimate state and cracking initiation and of the ultimate and cracking moment of the RC section. The equation considers the products of both ratios.

$$Z = \left(\frac{\Delta_u}{\Delta_{cr}} \right) \left(\frac{M_u}{M_{cr}} \right) \tag{5}$$

where Δ_u is the deflection at ultimate; Δ_α corresponds to the deflection at cracking initiation; M_{cr} corresponds to the cracking moment and M_u is the ultimate moment.

Lau and Pam [83], in experimentation with hybrid GFRP–steel RC, have partially introduced the conventional term of ductility index. In this approach, they redefined the term yield point (Δ_y), which refers to the nonlinear point of the beam's load–deflection curve. Lau and Pam [83] employed a new term μ as a dimensionless parameter given as:

$$\mu = \frac{\Delta_u}{\Delta_y} \tag{6}$$

where Δ_u and Δ_y are the midspan deflection at ultimate state and linear limit respectively.

A meaningful comparison among hybrid RC beams and other GFRP or steel-only reinforcements is made possible by Equation (7) developed by Pang et al. [101]. In this concept, the effective reinforcement area of GFRP will be converted into equivalent steel. The proposed ductility index μ_h is designed to satisfy the ductility requirements for conventional steel-reinforced concrete members.

$$\mu_h = \frac{\Psi D_{uh}}{D_{yh}} \geq [\mu_D] \tag{7}$$

$$\Psi = \frac{U_H}{U_S} \leq 1.0$$

where U_H expresses the area under the moment-curvature curve of the beam; U_s represents the area under the moment–curvature of the equivalent steel–RC beam; D_{uh} is the ultimate deformation of the beam; D_{yh} is the deformation of the beam at the beginning of steel yielding; Ψ expresses the ductility reduction factor; and μ_D is the ductility requirements based on the conventional indices.

Although the approaches proposed by these studies were able to compute the ductility of the hybrid RC components, none of them addressed the ductility activation phenomenon. Such information may be useful for understanding the behaviour of both the GFRP and steel reinforcements while designing flexural beams. A ductility model that clarifies the ductility activation phenomenon of the inner steel bar may be helpful information in developing a comprehensive design model for hybrid GFRP–steel RC systems.

3.1.2. Crack Width Analysis

The concrete structural elements are expected to develop cracks under service loads due to the concrete's inherent low tensile strength. As such, crack width calculation is one of the serviceability requirements of all structural concrete elements. The crack width evaluations are developed based on the durability of steel-reinforced concrete structures. Steel reinforcements embedded in the concrete structure are vulnerable to permeating electrolytes, and the crack networks are potential pathways to breach the barrier for transporting corroding agents [107]. Therefore, these crack limitation considerations are traditionally developed with a focus on steel-only RC elements.

With GFRP-only reinforced beams, there is no risk of corrosion. The Japan Society of Civil Engineers [108] therefore proposed disregarding the crack width limitations in the GFRP reinforced structural elements. On the other hand, building standards such as ACI [109] advocate guidelines to crack control in GFRP-reinforced structures. Models that give consideration to crack development may be more suited for hybrid GFRP–steel reinforcements because of the presence of steel bars that requires protection from corrosion. In other words, determining the width and development of cracks in hybrid GFRP–steel RCs is critical to avoiding corrosion damage and ensuring their durability.

The design recommendation by the American Association of State Highway and Transportation Officials (AASHTO) [110] gives limitations for crack width (w) as:

$$w = \frac{2\, d_c\, f_{fs}\, \xi}{C_b E_f} \tag{8}$$

Equation (8) establishes the crack limit is the product of the bond (reduction factor) (C_b) between GFRP reinforcing bars and surrounding concrete, the thickness of the concrete cover (d_c), the tensile modulus of the GFRP bar (E_f), the ratio of the distance from the neutral axis to extreme tensile zone (ξ), and calculated tensile stress in GFRP (f_{fs}). Other design standards such as ACI and CSA also give limitations similar to AASHTO, but these guidelines did not include the crack width limitations for hybrid systems.

The bond coefficient significantly influences and impacts on the accuracy of crack width predictions put forward by the design standards. Hence, researchers [110,111] developed predictive models that consider both GFRP and steel bars while designing hybrid RC elements.

Equation (9) provided by ACI-440.1R-06 [112,113] gives the maximum crack width limit in GFRP-reinforced concrete beams. Where σ_f represents reinforcement stress, E_f represents the modulus of elasticity rebar, d_c is the distance from the tension face to the centre of the closest bar, and is the bar spacing. It also recommends k_b as the bond coefficient that is primarily taken as 1.40 for GFRP-reinforced beams.

$$w = 2\frac{\sigma_f}{Ef}\, \beta k_b \sqrt{d_c^2 + \left(\frac{s}{2}\right)^2} \tag{9}$$

Experimental studies by Refai et al. [111] suggested the expression given in Equation (10) to estimate the bond coefficient, $k_{b,}$ for the hybrid GFRP–steel reinforced beams. It is evident from the work of Refai et al. [111] that k_b depends on the area ratio of GFRP (A_f) to that of steel (A_s) and is given as:

$$k_b = 1.4\alpha \left(\frac{A_f}{A_s}\right)^{\frac{1}{5}} \tag{10}$$

where α accounts for the size effect of GFRP bars on the embedded concrete interface, A_f and A_s are the areas of GFRP and steel reinforcements, respectively.

3.1.3. Flexure Modelling

Flexural strength is the intensity of force acting perpendicular to its longitudinal axis a beam can resist without ultimate failure. RC beams experience flexure and encounters dif-

ferent stress stages with the assumption of tensile-governed failure [114]. Implementation of GFRP reinforcement exclusively may result in beams exhibiting reduced flexural strength and brittle failure mode [23]. Hybrid GFRP–steel reinforcement systems are proposed to overcome these downsides [33]. In such hybrid systems, the characteristic plasticity of the steel contributes to the ductility of the RC beam, and the high tensile strength of the GFRP defines its ultimate load-bearing capacity [115]. Figure 6 depicts the moment-curvature ($M - \varphi$) curves of various flexural members with equivalent reinforcement areas [101].

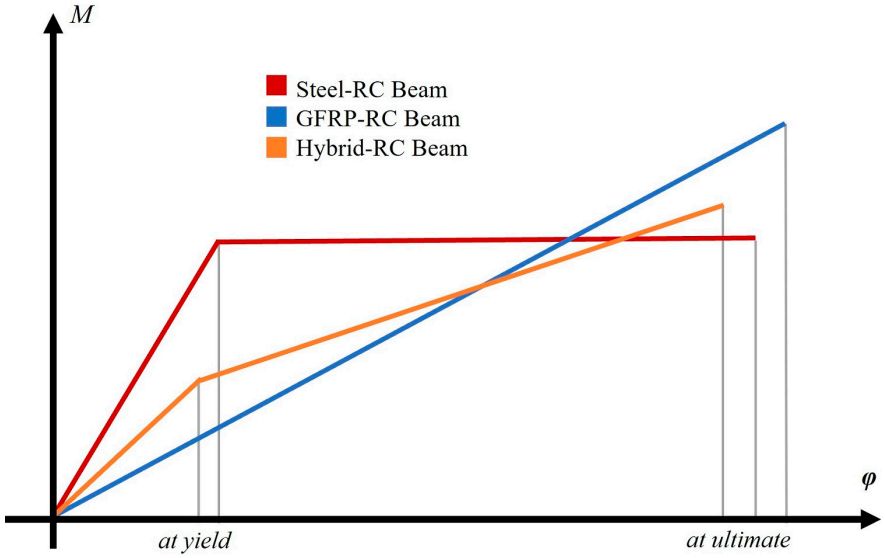


Figure 6. Moment–curvature for beams with different reinforcement systems [101]. Reproduced with permission from ASCE 2023.

Experimental studies on the flexure modelling of hybrid GFRP-steel RC beams are summarised in Table 2. It is seen that nearly all the beams tested failed due to steel yielding and concrete crushing. The investigations presented in Table 2, however, show the progress in developing the hybrid RC beams concept with under-reinforced beam characteristics. These studies have demonstrated the use of hybrid GFRP–steel reinforcement systems are effective in maintaining the required flexural responses. Furthermore, these studies are mostly based on the analytical models recommended in ACI standards that have been adjusted for hybrid beam designs. The altered design models are then calibrated and correlated with experimental results.

In general, the studies investigating the flexural behaviour of hybrid GFRP–steel RC beams summarised in Table 2 indicate distinct behaviour compared to conventional steel RC beams. The hybrid beam is characterised by a flexure–shear failure mode with narrower crack propagation. On the other hand, steel RC beams are normally characterised by wider crack widths when subjected to similar displacement and loading conditions. Additionally, for hybrid GFRP–steel RCs many of the rupture failure identified [43,85] are attributed to the shear failure between longitudinal reinforcement and concrete. This debonding lead to the formation of horizontal cracks in flexure beams.

Further analysis of the failure modes in studies is summarised in Table 2 and is visually represented in Figure 7. It is clear that a significant proportion (78%) of failure modes observed are from "steel yielding and concrete crushing" as shown in Figure 7. Only 3.1% is from "GFPR rupture". Data collection is from experiments conducted that have the beam specimen designed with additional shear reinforcements that restrict shear. This limited the gathering of information about the flexure–shear failure characteristics of the hybrid GFRP–steel RC beams.

Table 2. Overview of Tested Beams.

Source	Beam ID	Reinforcement Content			Reinforcement Type			Ultimate Moment (kNm)		Ultimate Load (kN)		Analytical Model Referenced	Failure Mode
		%		Combined (ρ)	Under	Over	Balanced	Experimental	Theoretical	Experimental	Theoretical		
		ρ_{eff}	$\rho_{eff.b}$										
[39]	B1	1.14	3.23			✓				107.9	108.9	ACI 440	SY, CC
	B2	0.29	-			✓				146.3	136.9		CC
	B3	0.71	3.45			✓				127.6	134.8		SY, CC
	B4	0.71	3.73			✓				132.2	145.4		SY, CC
	B5	1.08	3.88			✓				121.2	131.3		SY, CC
	B6	1.16	3.88			✓				141.9	155.1		SY, CC
	B7	0.35	4.08			✓				78.5	83.3		SY, CC
	B8	3.49	4.41			✓				211.0	272.8		SY, CC
[83]	MD 1.3	1.31	4.71		✓			147.4	127.1			BD 2004	SY, CC
	G 0.8	0.83	0.75				✓	158.8	142.2				RUP
	G 0.3	0.89	0.85				✓	147.0	143.2				SY, CC, RUP
	MD 2.1	2.07	5.27		✓			252.7	189.3				SY, CC
	G 2.1	2.07	0.69			✓		238.0	222.6				CC, RUP
	G 1.0	1.71	0.81			✓		261.0	216.5				SY, CC, RUP
	G 0.6	1.56	0.92			✓		229.0	228.2				SY, CC, RUP
[40]	S1	1.2	0.7			✓		72.5	81.3			ACI 440	CC
	S2	2.64	8.56		✓			69.9	80.3				SY, CC
	S3	2.64	8.56		✓			74.8	80.3				SY, CC
	S4	2.64	8.56		✓			82.0	80.3				SY, CC
[41]	B10/8S	n/a			✓					63.0	60.8	BS EN 197-1	SY, CC
	B10/8				✓					59.6	60.8		SY, CC
	B10/6S				✓					61.6	55.4		SY, CC
	B10/6				✓					58.8	55.4		SY, CC
	B12/8S				✓					71.4	66.1		SY, CC
	B12/8				✓					64.0	66.1		SY, CC
	B12/6S				✓					65.1	61.8		SY, CC
	B12/6				✓					61.4	61.8		SY, CC
[111]	G21S0	0.51	0.49			✓		47.62	47.27			CSA-S806-12	SY, CC, RUP
	G22S0	0.55	0.49			✓		53.55	58.43				SY, CC
	G22S2	0.67	0.49			✓		58.94	55.72				SY, CC
	G62S2	0.85	0.49			✓		68.30	71.41				SY, CC
	G62S2	0.96	0.49			✓		64.71	70.92				SY, CC
	G62S6	1.13	0.49			✓		83.53	81.39				SY, CC
[42]	G1.0T			1.71		✓				248.5	230.50	ACI 440	SY, CC
	G0.6T			1.56		✓				218.0	222.55		SY, CC
[43]	S2G21	n/a			n/a			133.0	127.8			AFGC/SETRA	CC
	S2G22							130.1	112.1				RUP
	S2G3							146.8	136.8				CC
	S3G3							161.3	146.0				CC
[84]	2S1G			0.84		✓				50.47	42.49	ATENA	SY, CC
	1S2G			0.89		✓				49.70	51.83		SY, CC
	3S2Ga			1.46		✓				67.38	67.55		SY, CC
	2S3Ga			1.51		✓				65.96	75.35		SY, CC
	3S2Gb			1.46		✓				66.01	67.55		SY, CC
	2S3Gb			1.51		✓				65.94	75.35		SY, CC
	4S2G			1.73		✓				76.11	75.64		SY, CC
	2S4G			1.83		✓				72.60	90.07		SY, CC

Table 2. *Cont.*

Source	Beam ID	Reinforcement Content			Reinforcement Type			Ultimate Moment (kNm)		Ultimate Load (kN)		Analytical Model Referenced	Failure Mode
		%		Combined (ρ)	Under	Over	Balanced	Experimental	Theoretical	Experimental	Theoretical		
		ρ_{eff}	$\rho_{eff.b}$										
[85]	CH1					✓		92.00	88.00			ACI 440	SY, CC
	CH2					✓		112.0	105.0				SY, CC
	CH3		n/a			✓		125.0	128.0				SY, CC
	CH4					✓		128.0	143.0				SY, CC
	CH5					✓		160.0	169.0				SY, CC
[86]	GG1S	0.95	0.25			✓		88.6	72.6			CSA	SY, CC
	G2G2S	1.18	0.25			✓		88.0	74.8				SY, CC
	G3G2S	1.57	0.25			✓		96.3	82.8				SY, CC
	S3G	1.18	0.25			✓		98.7	78.9				CC
	G3S	0.50	2.37		✓			67.2	65.18				SY
[87]	G2-S2	2.27	0.70					57.5	46.98			ACI 440	SY, CC
	G6-S2	2.27	0.72					63.3	56.56				SY, CC
	G2-S6	2.13	0.67					56.37	45.8				SY, CC
	G6-S6	2.13	0.69			n/a		66.7	55.78				SY, CC
	G2S2D	2.27	0.70					53.79	41.61				SY, CC
	G6S2D	2.27	0.72					50.56	50.69				SY, CC

SY—Steel Yielding, CC—Concrete Crushing, RUP—GFRP Rupture.

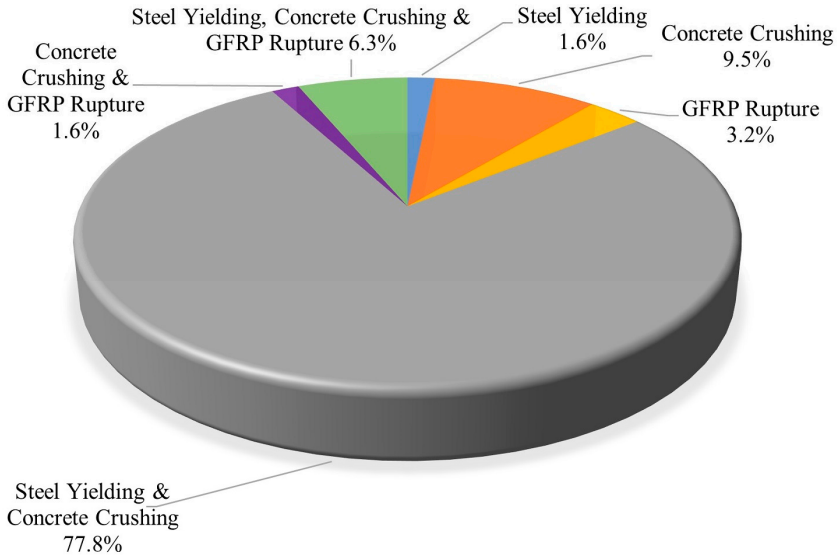


Figure 7. Distribution of failure modes in hybrid GFRP–steel beams reported in Table 2.

3.1.4. Shear Design

Generally, the shear resistance of the concrete member can be computed by using $V_{cf} + V_{sf}$ approach. It is also the most used and preferred approach. V_{cf} and V_{sf} refer to the shear strengths of the concrete and GFRP stirrups, respectively [116–119]. This method was developed on the basis of the strut-and-tie model [120,121], where the assumption was based on the modern truss model with parallel chords, vertical stirrup and constant inclination of 45^0 of the shear cracks [122,123].

The shear strength of RC beams is informed by the aggregate interlock, friction force along the shear crack, residual tensile strength, shear strength of the longitudinal reinforcement (dowel action) and the shear strength from the transverse reinforcement (stirrups) [124,125]. It was identified that the dowel capability of GFRP is about 70% lower than that of steel. Previous research has shown that V_{cf} is also influenced by the stiffness

of the tensile reinforcement [108,126,127]. As such, an overall reduction in V_{cf} could be expected when GFRPs are used for longitudinal reinforcement, as those bars produce a larger tensile strain [128].

Experimental studies observed a significant reduction in the ultimate capacity of GFRP bars when used as stirrups, with studies pointing out that the occurrence of failure initiated at the bends of the stirrups. It has been reported that the current design guidelines result in prescribing excessive shear reinforcement, making those procedures arguably very conservative [129–131].

Attempts have been made to fit GFRP characteristics in conventional design equations, and new rules have been introduced to derive modified versions of existing equations [132]. Table 3 shows the modification to design equations as published in various standards.

Table 3. Modifications to code design equations.

Source	V_{cf}	V_{sf}
[119]	$0.2 \cdot \sqrt[4]{\frac{1}{d}} \cdot \sqrt[3]{100 \cdot \frac{A_f}{b_w d} \frac{E_f}{E_s}} \cdot \sqrt[3]{f'_c} \cdot b_w \cdot d$	$\frac{A_{fw} \cdot E_{fw} \cdot \varepsilon_{fwd}}{S} \cdot Z$
[133]	$0.79 \cdot \left(\frac{100}{b_w \cdot d} \cdot A_f \cdot \frac{E_f}{200}\right)^{1/3} \cdot \left(\frac{400}{d}\right)^{1/4} \cdot \left(\frac{f_{cu}}{25}\right)^{1/3}$	$\frac{0.0025 E_{fw} \cdot A_{fw}}{b_w \cdot S}$
[116]	$0.4 \sqrt{f'_c}\, b_w c$	$\frac{A_{fw} f_{fw} d}{s}$
[134]	$0.035\, \lambda \left(f'_c \rho_f E_f \frac{V_f}{M_f} d\right)^{1/3} b_w d$	$\frac{0.4\ A_{fw} f_{fw} d}{s}$
[117]	$1.3 \left(\frac{E_f}{E_s}\right)^{1/2} \tau_{Rd} k \left(1.2 + 40 \rho_f\right) b_w d$	$\frac{A_{fw} f_{fw} d}{s}$
[135,136]	$0.12 \left(1 + \sqrt{\frac{200}{d}}\right) \left(100 \cdot \frac{A_f}{b_w d} \cdot \frac{E_f}{E_s} \cdot \varnothing_\varepsilon \cdot f_{ck}\right)^{1/3} b_w d$	$\frac{0.0025 E_{fw} \cdot z \cdot A_{fw}}{S}$
[135,137]	$0.79 \left(\frac{100}{b_w \cdot d} \cdot A_f \cdot \frac{E_f}{200} \cdot \varnothing_\varepsilon\right)^{1/3} \cdot \left(\frac{400}{d}\right)^{1/4} \cdot \left(\frac{f_{cu}}{25}\right)^{1/3} b_w d$	$\frac{0.0025 E_{fw} \cdot A_{fw}}{b_w \cdot S}$
[135,138]	$V_c \cdot \left(\frac{E_f}{E_s} \cdot \varnothing_\varepsilon\right)^{1/3}$	$\frac{0.0025 E_{fw} \cdot A_{fw}}{S}$

3.2. Models Considering Physical Effects: Fire Modelling

The fire resistance of an RC structural element is obtained by measuring the strength of an element as a function of the time required to attain its structural failure [139]. To ensure the appropriate fire performance of hybrid GFRP–steel RC structures, adequate information on concrete elements at elevated temperatures is indispensable [140]. Such information on concrete's thermo-mechanical properties are derived from data obtainable from the thermal analysis of cementitious binders.

The effect of temperature on the cementitious binder in concrete is well documented and generally visually represented with thermo-gravimetery (TG) and differential thermo-gravimetery (DTG). It is generally agreed that changes in Portland cement binder concrete observed at temperatures exceedingly ambient can be described in two stages [141] before the complete breakdown of the binding effect in mortar matrix in concrete. In the first stage (temperature range 22–120 °C) an increase in partial pressure caused by evaporative loss of absorbed water can cause some swelling but rarely is related to a significant loss of strength of the concrete matrix [142]. The second stage is typically at about 350 °C and is accompanied by a structural breakdown of the hydration reaction for the cement bond. This stage is typically represented by a sharp mass loss in a TG and a well-defined DTG peak [141]. Figure 8 shows the typical TG signal for some cementitious concrete binder phases. The gradual TG mass loss below 200 °C is consistent with evaporative water loss, and the sharp TG mass loss of about 20–30% between 300–400 °C represents the structural breakdown of the concrete binder. This sets the limits of maximum tolerable temperature for an RC load bearing system.

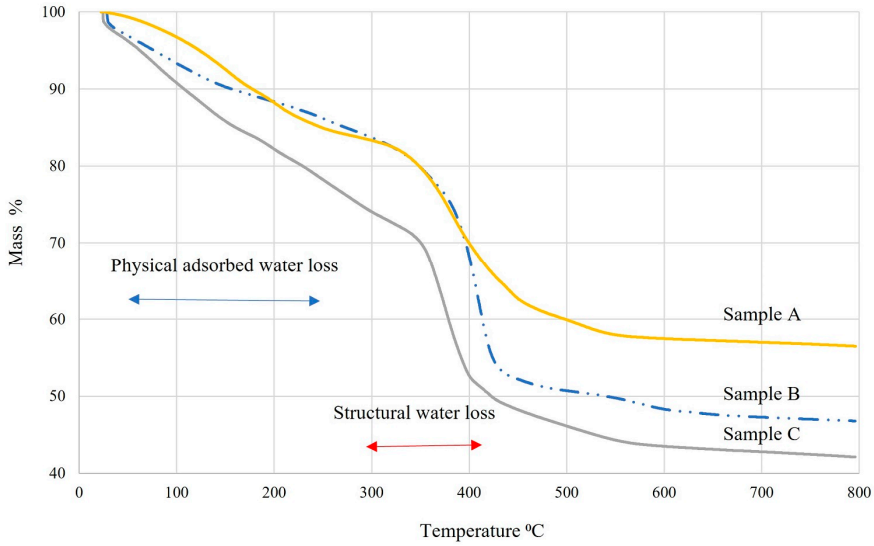


Figure 8. Thermogravimetric pattern of cementitious binder.

It generally takes up to 3 h for a fire's heat to go through a concrete member's cover and reach the reinforcement [143–145]. A recent study by Hajiloo et al. [146] have detailed fire effects on temperature gradients and demonstrated that a temperature of around 400 °C is obtainable at the 40 mm depth in a concrete zone within 3 h of exposure to a standard fire [147].

High fire resistance and low cost are significant advantages of using steel rebars in concrete structures [148], considering its temperature threshold is set to between 300 °C to 500 °C and its thermal expansion coefficient of 11.7 × 10^{-6}/°C [116,149,150]. In comparison, GFRP bars start to lose their flexural and bond strengths at temperatures above 120 °C. However, the complete thermal degradation of the polymer matrix can stand up to 350 °C. GFRP's load-bearing capability is therefore restricted to much lower temperatures compared to that of steel [151,152]. Furthermore, GFRP exhibit a non-uniform and highly variable coefficient of thermal expansion (8–33 × 10^{-6}/°C) depending on the direction. Along the longitudinal direction, the GFRP coefficient of thermal expansion is in the range 8–10.0 × 10^{-6}/°C [116] and is similar in magnitude to that of steel.

Finite element (FE) and experimental research have been performed to examine the fire behaviour of GFRP RC beams, but direct experimentation has been rather limited. The outcomes from these studies (summarised in Table 4), suggest that the concrete cover thickness has a significant role in the fire-resisting period of the elements. According to experimental tests, a minimum concrete cover of 65 mm is recommended to meet the standard required for a fireproofing of 90 min and impart adequate protection to the GFRP reinforcement. Such a thick cover is not economical and may deter to use of GFRP.

Additionally, fire retardant coating can provide a potential resistance for fibres from elevated temperatures [153,154]. A recent study conducted by M.H. Khaneghahi et al. [155] concluded that the fire-retardant coating helps to preserve the mechanical properties of the GFRP bars in the range of 350–600 °C, and even increases the tensile strength retention rate by 20–30%. A significant decrease on the performance of fire-retardant coating was only noted when the temperature exceeded 600 °C.

Moreover, the fire safety building regulations impose that the minimum period of fire resistance should be 90 min [156]. Meanwhile, most standard procedures of concrete structure fireproofing recommend a cover thickness that should provide a fire resistance of 90 min with exposure to a peak temperature of 350 °C. GFRP reinforcement would therefore be adequate for most categories of buildings and structures.

Table 4. Overview of FE and Experimental studies.

Literature	Fire Resistance Time t (Min)	Concrete Cover (mm)	Peak Temperature (°C)	Specimen Model	Fire Model
[157]	60	64	400	ENV EC2-1992	ASTM E119-1976
[158]	94	70	377	ENV EC2-1992 ACI-440-2001	BS 476-1987
[159]	30	50	400	ENV EC2-1992 (Hybrid Steel)	-
[160]	45	25	160	ISIS Canada-2001	ASTM E119 ISO 834
[148]	90	85	225	-	DIN EN 1363
[161]	60	20	170	ACI 440.1R-06	BS EN 1363-1
[162]	50	20	820	1-D two-node Composite Beam Element	ISO 834
[163]	120	70	400	3-D nonlinear FE Model	ISO 834
[164]	40	30	500	ENV EC2-1992	EC1

4. Outlook for Future

The existing research and engineering practices overviewed in this paper elaborate on the huge potential of hybrid GFRP–steel reinforcement systems to meet the durability, strength, and serviceability requirements of most civil engineering applications. The studies agree on the superiority of GFRP rebars in their tensile strength and durability compared to steel reinforcement. Moreover, the hybrid application of GFRP and steel is an effective way to develop ductile responses to GFRP-reinforced beams. However, there is a lack of understanding in specifying and defining the ductility activation in the hybrid GFRP–steel beam systems. A few concepts already exist, but further research is needed to enable the scalability and generalisation of the proposed models. This section discusses these constraints, challenges, and the outlook for future research.

The concept of hybrid GFRP–steel reinforcement is still in its developing stage. The available research data and information from the out-of-the-lab implementation are building up. There is, however, great need to better understand and predict the failure modes and ultimate states of hybrid reinforcements.

There is a lot to learn about the concept of ductility, its development and its application to hybrid GFRP-steel RC systems. Whilst many of the proposed design models of hybrid GFRP-steel beams are anticipated to develop into ductile failure modes, these models have been developed based on steel RCs and their calibration conducted with set ratios and the arrangements of reinforcement bars.

This lack of detailed information on different areas calls for more clarification before the application of GFRP–steel hybrid RC systems can become practice. Hence, the following summarises the topics of interest for future research studies.

- Investigation of the factors that control the activation of ductile behaviour in steel reinforcement in hybrid reinforcement arrangements.
- Experimental studies on GFRP shear reinforcement (stirrups) incorporated with hybrid reinforcement systems.
- Experimental and numerical studies on the effects of different grades of steel on ductility development in hybrid GFRP–steel RC beams.
- Investigation of the behaviours of hybrid GFRP-steel reinforcement systems to varying temperature gradients and their recovery.
- Investigations on the long-term durability of GFRP bars.

- Numerical modelling of the effects of bond-slip behaviour of GFRP in hybrid RC systems.
- Experimental and numerical studies of the effects of the surface characteristics of GFRP bars on the structural performance of hybrid RC beams.

5. Conclusions

GFRP reinforcements are a potential alternative to steel rebars for durable and corrosion-free structures. Though design codes exist for the use of GFRP in RCs, there is scope to address their lack of ductility with the addition of steel reinforcement. This paper has overviewed the research carried out to advance the design of a hybrid GFRP–steel reinforcement system for concrete beams. The primary focus was given to the studies conducted on analytical models that considered mechanical and physical effects to enhance the performance of flexure beams. The main conclusions are summarised as follows:

- The inherent corrosive nature of steel is a threat to the durability of RC structures, specifically in aggressive environments. The FRPs, which has high strength-to-weight ratio than steel, are one of the most suitable solution to enhance the durability of RC structures.
- GFRP is an economically viable option for the usual commercial applications. Although its properties are not as competent as other FRP variants such as CFRP and BFRP, it is proven to be more efficient than using conventional steel bars, especially in harsh environments.
- Lack of ductility is one of the characteristic traits that questions the application of GFRP bars in flexure beams, where flexural yield is a demanding behaviour to design safe structures. Despite proposing new parameters to quantify the ductility of GFRP-steel RC beams, the studies explaining the synergetic mechanism between the GFRP and steel is very limited.
- The crack developments in the hybrid beams are highly dependable on the bond coefficient used in the design. Hence, it is important to understand the bond behaviour between the GFRP bars used in the hybrid system.
- Most of the flexural beams that experimented with the GFRP–steel hybrid reinforcement system has reported a combined failure mode of steel yielding and concrete crushing. This indicates the activation of the yield behaviour of steel bars before the (rupture) failure of GFRP in the system, which gives the confidence to consider a hybrid reinforcement system for flexure beams.
- In the experimental studies of hybrid GFRP–steel, excessive shear reinforcement has been employed as a strategy to prevent shear failure.
- The attempt to engineer the shear response of hybrid GFRP–steel in RC led to a notable improvement in the performance of flexure-shear failures with a minimal amount of shear cracks and shear crack widths.
- The weakness of GFRPs in RC is in its susceptibility to thermal degradation at comparatively lower temperatures than steel. However, recent studies suggested that this weakness can be mitigated by using adequate concrete cover for increased thermal resistance and applying fire retardants to enhance its performance up to the recommended standard.
- Hybrid GFRP–steel reinforcement is an effective and competitive alternative to steel reinforcement. As identified in this paper, key aspects of their design and structural behaviours must be better understood and require further research to put forward a reliable and sound design procedure.

Author Contributions: Conceptualization, R.D.; Supervision, C.G. and A.O.; data curation, R.D., A.O. and C.G.; writing—review and editing, A.O. and C.G.; writing—original draft preparation, R.D. All authors have read and agreed to the published version of the manuscript.

Funding: This research received no external funding.

Institutional Review Board Statement: Not applicable.

Informed Consent Statement: Not applicable.

Data Availability Statement: Not applicable.

Conflicts of Interest: The authors declare no conflict of interest.

References

1. Attia, M.M.; Ahmed, O.; Kobesy, O.; Malek, A.S. Behavior of FRP rods under uniaxial tensile strength with multiple materials as an alternative to steel rebar. *Case Stud. Constr. Mater.* **2022**, *17*, e01241. [CrossRef]
2. Looney, T.; Leggs, M.; Volz, J.; Floyd, R. Durability and corrosion resistance of ultra-high performance concretes for repair. *Constr. Build. Mater.* **2022**, *345*, 128238. [CrossRef]
3. Ming, J.; Zhou, X.; Jiang, L.; Shi, J. Corrosion resistance of low-alloy steel in concrete subjected to long-term chloride attack: Characterization of surface conditions and rust layers. *Corros. Sci.* **2022**, *203*, 110370. [CrossRef]
4. Yu, X.; Al-Saadi, S.; Zhao, X.L.; Raman, R.K.S. Electrochemical investigations of steels in seawater sea sand concrete environments. *Materials* **2021**, *14*, 5713. [CrossRef] [PubMed]
5. Melchers, R.E.; Chaves, I.A. Durable steel-reinforced concrete structures for marine environments. *Sustainability* **2021**, *13*, 13695. [CrossRef]
6. Němeček, J.; Trávníček, P.; Němečková, J.; Kruis, J. Mitigation of chloride induced corrosion in reinforced concrete structures and its modeling. *Koroze A Ochr. Mater.* **2021**, *65*, 79–85. [CrossRef]
7. Omer, L.M.; Gomaa, M.S.; Sufe, W.H.; Elsayed, A.A.; Elghazaly, H.A. Enhancing corrosion resistance of RC pipes using geopolymer mixes when subjected to aggressive environment. *J. Eng. Appl. Sci.* **2022**, *69*, 3. [CrossRef]
8. Li, W.; Wu, M.; Shi, T.; Yang, P.; Pan, Z.; Liu, W.; Liu, J.; Yang, X. Experimental Investigation of the Relationship between Surface Crack of Concrete Cover and Corrosion Degree of Steel Bar Using Fractal Theory. *Fractal Fract.* **2022**, *6*, 325. [CrossRef]
9. Li, Q.; Gao, Z.; Yang, T.; Dong, Z.; Jiang, Z.; He, Q.; Fu, C. Rust Distribution of Non-Uniform Steel Corrosion Induced by Impressed Current Method. *Materials* **2022**, *15*, 4276. [CrossRef]
10. Gao, X.X.; Deby, F.; Gourbeyre, Y.; Samson, G.; Garcia, S.; Arliguie, G. Influence of catholytes on the generation of steel corrosion in concrete with accelerated chloride migration method. *Case Stud. Constr. Mater.* **2022**, *16*, e01123. [CrossRef]
11. Schmitt, G. Global needs for knowledge dissemination, research, and development in materials deterioration and corrosion control. *World Corros. Organ.* **2009**, *38*, 14.
12. Mohammed, T.U.; Rahman, M.; Sabbir, A.; Hasan, M.M.; Mamun, A.A. Chloride ingress and macro-cell corrosion of steel in concrete made with recycled brick aggregate. *Front. Struct. Civ. Eng.* **2021**, *15*, 1358–1371. [CrossRef]
13. O'Reilly, M.; Darwin, D.; Browning, J.; Locke, C.E.; Virmani, Y.P.; Ji, J.; Gong, L.; Guo, G.; Draper, J.; Xing, L. Multiple Corrosion Protection Systems for Reinforced Concrete Bridge Components: Field Tests. *J. Mater. Civ. Eng.* **2021**, *33*, 04021363. [CrossRef]
14. Long, Z.; Zhang, R.; Wang, Q.; Xie, C.; Zhang, J.; Duan, Y. Mechanism analysis of strength evolution of concrete structure in saline soil area based on 15-year service. *Constr. Build. Mater.* **2022**, *332*, 127281. [CrossRef]
15. Hassanli, R.; Youssf, O.; Manalo, A.; Najafgholipour, M.A.; Elchalakani, M.; Del Rey Castillo, E.; Lutze, D. An Experimental Study of the Behavior of GFRP-Reinforced Precast Concrete Culverts. *J. Compos. Constr.* **2022**, *26*, 04022043. [CrossRef]
16. Sheikh, S.A.; Kharal, Z. Replacement of steel with GFRP for sustainable reinforced concrete. *Constr. Build. Mater.* **2018**, *160*, 767–774. [CrossRef]
17. Jabbar, S.A.; Farid, S.B. Replacement of steel rebars by GFRP rebars in the concrete structures. *Karbala Int. J. Mod. Sci.* **2018**, *4*, 216–227. [CrossRef]
18. El-Sayed, T.A.; Erfan, A.M.; Abdelnaby, R.M.; Soliman, M.K. Flexural behavior of HSC beams reinforced by hybrid GFRP bars with steel wires. *Case Stud. Constr. Mater.* **2022**, *16*, e01054. [CrossRef]
19. Karim, R.; Shafei, B. Performance of fiber-reinforced concrete link slabs with embedded steel and GFRP rebars. *Eng. Struct.* **2021**, *229*, 111590. [CrossRef]
20. Ramanathan, S.; Benzecry, V.; Suraneni, P.; Nanni, A. Condition assessment of concrete and glass fiber reinforced polymer (GFRP) rebar after 18 years of service life. *Case Stud. Constr. Mater.* **2021**, *14*, e00494. [CrossRef]
21. Li, W.; Wen, F.; Zhou, M.; Liu, F.; Jiao, Y.; Wu, Q.; Liu, H. Assessment and Prediction Model of GFRP Bars' Durability Performance in Seawater Environment. *Buildings* **2022**, *12*, 127. [CrossRef]
22. Wu, W.; He, X.; Yang, W.; Dai, L.; Wang, Y.; He, J. Long-time durability of GFRP bars in the alkaline concrete environment for eight years. *Constr. Build. Mater.* **2022**, *314*, 125573. [CrossRef]
23. Xingyu, G.; Yiqing, D.; Jiwang, J. Flexural behavior investigation of steel-GFRP hybrid-reinforced concrete beams based on experimental and numerical methods. *Eng. Struct.* **2020**, *206*, 110117. [CrossRef]
24. Acciai, A.; D'Ambrisi, A.; De Stefano, M.; Feo, L.; Focacci, F.; Nudo, R. Experimental response of FRP reinforced members without transverse reinforcement: Failure modes and design issues. *Compos. Part B Eng.* **2016**, *89*, 397–407. [CrossRef]
25. Li, L.; Lu, J.; Fang, S.; Liu, F.; Li, S. Flexural study of concrete beams with basalt fibre polymer bars. *Proc. Inst. Civ. Eng.-Struct. Build.* **2018**, *171*, 505–516. [CrossRef]

26. Yoo, D.-Y.; Moon, D.-Y. Effect of steel fibers on the flexural behavior of RC beams with very low reinforcement ratios. *Constr. Build. Mater.* **2018**, *188*, 237–254. [CrossRef]
27. Qin, F.; Zhang, Z.; Yin, Z.; Di, J.; Xu, L.; Xu, X. Use of high strength, high ductility engineered cementitious composites (ECC) to enhance the flexural performance of reinforced concrete beams. *J. Build. Eng.* **2020**, *32*, 101746. [CrossRef]
28. Deng, M.; Zhang, M.; Zhu, Z.; Ma, F. Deformation capacity of over-reinforced concrete beams strengthened with highly ductile fiber-reinforced concrete. In *Structures*; Elsevier: Amsterdam, The Netherlands, 2021; pp. 1861–1873.
29. Abbas, H.; Abadel, A.; Almusallam, T.; Al-Salloum, Y. Experimental and analytical study of flexural performance of concrete beams reinforced with hybrid of GFRP and steel rebars. *Eng. Fail. Anal.* **2022**, *138*, 106397. [CrossRef]
30. Yuan, J.; Gao, D.; Zhang, Y.; Zhu, H. Improving Ductility for Composite Beams Reinforced with GFRP Tubes by Using Rebars/Steel Angles. *Polymers* **2022**, *14*, 551. [CrossRef]
31. Xu, J.; Zhu, P.; Qu, W. Numerical and Analytical Study of Concrete Beams Reinforced with Hybrid Fiber-Reinforced Polymer and Steel Bars. *J. Compos. Constr.* **2022**, *26*, 04022045. [CrossRef]
32. Han, S.; Fan, C.; Zhou, A.; Ou, J. Simplified implementation of equivalent and ductile performance for steel-FRP composite bars reinforced seawater sea-sand concrete beams: Equal-stiffness design method. *Eng. Struct.* **2022**, *266*, 114590. [CrossRef]
33. Thamrin, R.; Zaidir, Z.; Iwanda, D. Ductility Estimation for Flexural Concrete Beams Longitudinally Reinforced with Hybrid FRP–Steel Bars. *Polymers* **2022**, *14*, 1017. [CrossRef] [PubMed]
34. Nguyen, P.D.; Dang, V.H.; Vu, N.A. Performance of concrete beams reinforced with various ratios of hybrid GFRP/steel bars. *Civ. Eng. J.* **2020**, *6*, 1652–1669. [CrossRef]
35. Moolaei, S.; Sharbatdar, M.K.; Kheyroddin, A. Experimental evaluation of flexural behavior of HPFRCC beams reinforced with hybrid steel and GFRP bars. *Compos. Struct.* **2021**, *275*, 114503. [CrossRef]
36. Li, Z.; Khennane, A.; Hazell, P.J.; Remennikov, A.M. Performance of a hybrid GFRP-concrete beam subject to low-velocity impacts. *Compos. Struct.* **2018**, *206*, 425–438. [CrossRef]
37. Sijavandi, K.; Sharbatdar, M.K.; Kheyroddin, A. Experimental evaluation of flexural behavior of high-performance fiber reinforced concrete beams using GFRP and high strength steel bars. In *Structures*; Elsevier: Amsterdam, The Netherlands, 2021; pp. 4256–4268.
38. Xiao, S.-H.; Lin, J.-X.; Li, L.-J.; Guo, Y.-C.; Zeng, J.-J.; Xie, Z.-H.; Wei, F.-F.; Li, M. Experimental study on flexural behavior of concrete beam reinforced with GFRP and steel-fiber composite bars. *J. Build. Eng.* **2021**, *43*, 103087. [CrossRef]
39. Qu, W.; Zhang, X.; Huang, H. Flexural behavior of concrete beams reinforced with hybrid (GFRP and steel) bars. *J. Compos. Constr.* **2009**, *13*, 350–359. [CrossRef]
40. Liu, Y.H.; Yuan, Y. Experimental Studies on High Strength Concrete Beams Reinforced with Steel and GFRP Rebars. In *Applied Mechanics and Materials*; Trans Tech Publications Ltd.: Bäch, Switzerland, 2012; pp. 669–673.
41. Safan, M.A. Flexural Behavior and Design of Steel-GFRP Reinforced Concrete Beams. *ACI Mater. J.* **2013**, *110*, 667.
42. Qin, R.; Zhou, A.; Lau, D. Effect of reinforcement ratio on the flexural performance of hybrid FRP reinforced concrete beams. *Compos. Part B Eng.* **2017**, *108*, 200–209. [CrossRef]
43. Yoo, D.-Y.; Banthia, N.; Yoon, Y.-S. Flexural behavior of ultra-high-performance fiber-reinforced concrete beams reinforced with GFRP and steel rebars. *Eng. Struct.* **2016**, *111*, 246–262. [CrossRef]
44. Behera, P.K.; Misra, S.; Mondal, K. Corrosion of Strained Plain Rebar in Chloride-Contaminated Mortar and Novel Approach to Estimate the Corrosion Amount from Rust Characterization. *J. Mater. Civ. Eng.* **2021**, *33*, 04021283. [CrossRef]
45. Ding, Q.; Gao, Y.; Hou, W.; Qin, Y. Influence of Cl- concentration on corrosion behavior of reinforced concrete in soil. *J. Chin. Soc. Corros. Prot.* **2021**, *41*, 705–711. [CrossRef]
46. Ding, Q.; Gao, Y.; Liu, R.; Li, Y.; Jin, L.; Ma, H. Corrosion behavior of HRB400 and HRB400M steel bars in concrete under DC interference. *Sci. Rep.* **2021**, *11*, 23871. [CrossRef] [PubMed]
47. Franco-Luján, V.A.; Maldonado-García, M.A.; Mendoza-Rangel, J.M.; Montes-García, P. Effect of Cl−-induced corrosion on the mechanical properties of reinforcing steel embedded in ternary concretes containing FA and UtSCBA. *Constr. Build. Mater.* **2022**, *339*, 127655. [CrossRef]
48. Alexander, M.; Beushausen, H. Durability, service life prediction, and modelling for reinforced concrete structures–review and critique. *Cem. Concr. Res.* **2019**, *122*, 17–29. [CrossRef]
49. Afshar, A.; Shokrgozar, A.; Afshar, A.; Afshar, A. Simulation of corrosion protection methods in reinforced concrete by artificial neural networks and fuzzy logic. *J. Electrochem. Sci. Eng.* **2022**, *12*, 511–527. [CrossRef]
50. Bastidas, D.M.; Martin, U.; Bastidas, J.M.; Ress, J. Corrosion inhibition mechanism of steel reinforcements in mortar using soluble phosphates: A critical review. *Materials* **2021**, *14*, 6168. [CrossRef]
51. El Alami, E.; Fekak, F.E.; Garibaldi, L.; Elkhalfi, A. A numerical study of pitting corrosion in reinforced concrete structures. *J. Build. Eng.* **2021**, *43*, 102789. [CrossRef]
52. Fan, L.; Teng, L.; Tang, F.; Khayat, K.H.; Chen, G.; Meng, W. Corrosion of steel rebar embedded in UHPC beams with cracked matrix. *Constr. Build. Mater.* **2021**, *313*, 125589. [CrossRef]
53. Ge, W.J.; Zhu, J.W.; Ashour, A.; Yang, Z.P.; Cai, X.N.; Yao, S.; Yan, W.H.; Cao, D.F.; Lu, W.G. Effect of Chloride Corrosion on Eccentric-Compression Response of Concrete Columns Reinforced with Steel-FRP Composite Bars. *J. Compos. Constr.* **2022**, *26*, 04022042. [CrossRef]

54. Jee, A.A.; Pradhan, B. Long term effect of chloride and sulfates concentration, and cation allied with sulfates on corrosion performance of steel-reinforced in concrete. *J. Build. Eng.* **2022**, *56*, 104813. [CrossRef]
55. Graham-Jones, J.; Summerscales, J. *Marine Applications of Advanced Fibre-Reinforced Composites*; Woodhead Publishing: Sawston, UK, 2015.
56. Kim, Y.J. State of the practice of FRP composites in highway bridges. *Eng. Struct.* **2019**, *179*, 1–8. [CrossRef]
57. Noël, M. Probabilistic fatigue life modelling of FRP composites for construction. *Constr. Build. Mater.* **2019**, *206*, 279–286. [CrossRef]
58. Ferdous, W.; Manalo, A.; Sharda, A.; Bai, Y.; Ngo, T.D.; Mendis, P. Construction Industry Transformation through Modular Methods. In *Innovation in Construction*; Springer: Berlin/Heidelberg, Germany, 2022; pp. 259–276.
59. Li, C.; Zhu, H.; Niu, G.; Cheng, S.; Gu, Z.; Yang, L. Flexural behavior and a new model for flexural design of concrete beams hybridly reinforced by continuous FRP bars and discrete steel fibers. In *Structures*; Elsevier: Amsterdam, The Netherlands, 2022; pp. 949–960.
60. Davids, W.G.; Diba, A.; Dagher, H.J.; Guzzi, D.; Schanck, A.P. Development, assessment and implementation of a novel FRP composite girder bridge. *Constr. Build. Mater.* **2022**, *340*, 127818. [CrossRef]
61. Shin, J.; Park, S. Optimum retrofit strategy of FRP column jacketing system for non-ductile RC building frames using artificial neural network and genetic algorithm hybrid approach. *J. Build. Eng.* **2022**, *57*, 104919. [CrossRef]
62. George, J.M.; Kimiaei, M.; Elchalakani, M.; Efthymiou, M. Flexural response of underwater offshore structural members retrofitted with CFRP wraps and their performance after exposure to real marine conditions. In *Structures*; Elsevier: Amsterdam, The Netherlands, 2022; pp. 559–573.
63. Zhou, S.; Demartino, C.; Xu, J.; Xiao, Y. Effectiveness of CFRP seismic-retrofit of circular RC bridge piers under vehicular lateral impact loading. *Eng. Struct.* **2021**, *243*, 112602. [CrossRef]
64. Burgoyne, C.; Byars, E.; Guadagnini, M.; Manfredi, G.; Neocleous, K.; Pilakoutas, K.; Taerwe, L.; Taranu, N.; Tepfers, R.; Weber, A. *FRP Reinforcement in RC Structures*; FIB (International Federation for Structural Concrete): Losanna, Switzerland, 2007.
65. Coricciati, A.; Corvaglia, P.; Mosheyev, G. Durability of fibers in aggressive alkaline environment. In Proceedings of the 17th International Conference on Composite Materials-ICCM-17, Edinburgh, Scotland, UK, 27–31 July 2009.
66. Abbood, I.S.; aldeen Odaa, S.; Hasan, K.F.; Jasim, M.A.J. Properties evaluation of fiber reinforced polymers and their constituent materials used in structures—A review. *Mater. Today Proc.* **2021**, *43*, 1003–1008. [CrossRef]
67. Gooranorimi, O.; Nanni, A. GFRP reinforcement in concrete after 15 years of service. *J. Compos. Constr.* **2017**, *21*, 04017024. [CrossRef]
68. Gauvin, F.; Robert, M. Durability study of vinylester/silicate nanocomposites for civil engineering applications. *Polym. Degrad. Stab.* **2015**, *121*, 359–368. [CrossRef]
69. Bonsu, A.O.; Liang, W.; Mensah, C.; Yang, B. Assessing the mechanical behavior of glass and basalt reinforced vinyl ester composite under artificial seawater environment. In *Structures*; Elsevier: Amsterdam, The Netherlands, 2022; pp. 961–978.
70. Mukhtar, F.M.; Arowojolu, O. Recent developments in experimental and computational studies of hygrothermal effects on the bond between FRP and concrete. *J. Reinf. Plast. Compos.* **2020**, *39*, 422–442. [CrossRef]
71. Wang, P.; Wu, H.-L.; Leung, C.K. Mechanical and long-term durability prediction of GFRP rebars with the adoption of low-pH CSA concrete. *Constr. Build. Mater.* **2022**, *346*, 128444. [CrossRef]
72. Li, C.; Guo, R.; Xian, G.; Li, H. Effects of elevated temperature, hydraulic pressure and fatigue loading on the property evolution of a carbon/glass fiber hybrid rod. *Polym. Test.* **2020**, *90*, 106761. [CrossRef]
73. Lal, H.M.; Uthaman, A.; Li, C.; Xian, G.; Thomas, S. Combined effects of cyclic/sustained bending loading and water immersion on the interface shear strength of carbon/glass fiber reinforced polymer hybrid rods for bridge cable. *Constr. Build. Mater.* **2022**, *314*, 125587. [CrossRef]
74. Barcikowski, M.; Lesiuk, G.; Czechowski, K.; Duda, S. Static and flexural fatigue behavior of GFRP pultruded rebars. *Materials* **2021**, *14*, 297. [CrossRef]
75. Oskouei, A.V.; Bazli, M.; Ashrafi, H.; Imani, M. Flexural and web crippling properties of GFRP pultruded profiles subjected to wetting and drying cycles in different sea water conditions. *Polym. Test.* **2018**, *69*, 417–430. [CrossRef]
76. Wang, Z.; Zhao, X.-L.; Xian, G.; Wu, G.; Raman, R.S.; Al-Saadi, S. Effect of sustained load and seawater and sea sand concrete environment on durability of basalt-and glass-fibre reinforced polymer (B/GFRP) bars. *Corros. Sci.* **2018**, *138*, 200–218. [CrossRef]
77. Deitz, D.; Harik, I.; Gesund, H. Physical properties of glass fiber reinforced polymer rebars in compression. *J. Compos. Constr.* **2003**, *7*, 363–366. [CrossRef]
78. Choi, E.; Utui, N.; Kim, H.S. Experimental and analytical investigations on debonding of hybrid FRPs for flexural strengthening of RC beams. *Compos. Part B Eng.* **2013**, *45*, 248–256. [CrossRef]
79. Alraie, A.; Garg, N.; Matsagar, V.; Goldack, A.; Schlaich, M. Pseudo-Ductility through Progressive Failure of Multi-Layered Carbon-Fiber-Reinforced Polymer (CFRP) Prestressed Concrete Beams. *Struct. Eng. Int.* **2022**, 1–16. [CrossRef]
80. Askar, M.K.; Hassan, A.F.; Al-Kamaki, Y.S. Flexural and Shear Strengthening of Reinforced Concrete Beams Using FRP Composites: A State of The Art. *Case Stud. Constr. Mater.* **2022**, *17*, e01189. [CrossRef]
81. Harris, H.G.; Somboonsong, W.; Ko, F.K. New ductile hybrid FRP reinforcing bar for concrete structures. *J. Compos. Constr.* **1998**, *2*, 28–37. [CrossRef]

82. Issa, M.S.; Metwally, I.M.; Elzeiny, S.M. Influence of fibers on flexural behavior and ductility of concrete beams reinforced with GFRP rebars. *Eng. Struct.* **2011**, *33*, 1754–1763. [CrossRef]
83. Lau, D.; Pam, H.J. Experimental study of hybrid FRP reinforced concrete beams. *Eng. Struct.* **2010**, *32*, 3857–3865. [CrossRef]
84. Salleh, N.; Hamid, N.A.; Majid, M.A. Finite element modelling of concrete beams reinforced with hybrid fiber reinforced bars. In Proceedings of the Materials Science and Engineering Conference Series, Birmingham, UK, 13–15 October 2017; p. 012093.
85. Araba, A.M.; Ashour, A.F. Flexural performance of hybrid GFRP-Steel reinforced concrete continuous beams. *Compos. Part B Eng.* **2018**, *154*, 321–336. [CrossRef]
86. Maranan, G.; Manalo, A.; Benmokrane, B.; Karunasena, W.; Mendis, P.; Nguyen, T. Flexural behavior of geopolymer-concrete beams longitudinally reinforced with GFRP and steel hybrid reinforcements. *Eng. Struct.* **2019**, *182*, 141–152. [CrossRef]
87. Ruan, X.; Lu, C.; Xu, K.; Xuan, G.; Ni, M. Flexural behavior and serviceability of concrete beams hybrid-reinforced with GFRP bars and steel bars. *Compos. Struct.* **2020**, *235*, 111772. [CrossRef]
88. American Concrete Institute (ACI). *Guide for the Design and Construction of Structural Concrete Reinforced with Fiber Reinforced Polymer (FRP) Bars. 440.1 R-15*; American Concrete Institute: Farmington Hills, MI, USA, 2015.
89. Ge, W.; Wang, Y.; Ashour, A.; Lu, W.; Cao, D. Flexural performance of concrete beams reinforced with steel–FRP composite bars. *Arch. Civ. Mech. Eng.* **2020**, *20*, 1–17. [CrossRef]
90. Zhou, Y.; Wu, Y.; Teng, J.; Leung, A. Ductility analysis of compression-yielding FRP-reinforced composite beams. *Cem. Concr. Compos.* **2009**, *31*, 682–691. [CrossRef]
91. Oudah, F.; El-Hacha, R. Ductility of FRP reinforced RC structures: A critical review of definition and expressions. *Concr. Solut.* **2014**, *2014*, 329–335.
92. Bui, L.V.H.; Stitmannaithum, B.; Ueda, T. Ductility of concrete beams reinforced with both fiber-reinforced Polymer and steel tension bars. *J. Adv. Concr. Technol.* **2018**, *16*, 531–548. [CrossRef]
93. Newhook, J. Design of under-reinforced concrete T-sections with GFRP reinforcement. In *Proc., 3rd Int. Conf. on Advanced Composite Materials in Bridges and Structures*; Canadian Society for Civil Engineering: Montreal, QC, Canada, 2000; pp. 153–160.
94. Aiello, M.A.; Ombres, L. Structural performances of concrete beams with hybrid (fiber-reinforced polymer-steel) reinforcements. *J. Compos. Constr.* **2002**, *6*, 133–140. [CrossRef]
95. Ge, W.; Zhang, J.; Cao, D.; Tu, Y. Flexural behaviors of hybrid concrete beams reinforced with BFRP bars and steel bars. *Constr. Build. Mater.* **2015**, *87*, 28–37. [CrossRef]
96. Grace, N.F.; Soliman, A.; Abdel-Sayed, G.; Saleh, K. Behavior and ductility of simple and continuous FRP reinforced beams. *J. Compos. Constr.* **1998**, *2*, 186–194. [CrossRef]
97. Naaman, A.; Jeong, S. Structural Ductility of Concrete Beams Prestressed with FRP Tendons. In *Non-Metallic (FRP) Reinforcement for Concrete Structures: Proceedings of the Second International RILEM Symposium*; CRC Press: Boca Raton, FL, USA, 1995; p. 379.
98. Abdelrahman, A.; Tadros, G.; Rizkalla, S. Test model for first canadian smart highway bridge. *ACI Struct. J.* **1995**, *92*, 451–458.
99. Zou, P.X. Flexural behavior and deformability of fiber reinforced polymer prestressed concrete beams. *J. Compos. Constr.* **2003**, *7*, 275–284. [CrossRef]
100. Shin, S.; Seo, D.; Han, B. Performance of concrete beams reinforced with GFRP bars. *J. Asian Archit. Build. Eng.* **2009**, *8*, 197–204. [CrossRef]
101. Pang, L.; Qu, W.; Zhu, P.; Xu, J. Design propositions for hybrid FRP-steel reinforced concrete beams. *J. Compos. Constr.* **2016**, *20*, 04015086. [CrossRef]
102. El Zareef, M.A.; El Madawy, M.E. Effect of glass-fiber rods on the ductile behaviour of reinforced concrete beams. *Alex. Eng. J.* **2018**, *57*, 4071–4079. [CrossRef]
103. Abdelrahman, A.A.; Rizkalla, S.H. Serviceability of concrete beams prestressed by carbon. *ACI Struct. J.* **1997**, *94*, 447–454.
104. Mufti, A.A.; Newhook, J.P.; Tadros, G. Deformability versus ductility in concrete beams with FRP reinforcement. In Proceedings of the 2nd International Conference on Advanced Composite Materials in Bridge and Structures, Montreal, QC, Canada, 11–14 August 1996.
105. Bakht, B.; Al-Bazi, G.; Banthia, N.; Cheung, M.; Erki, M.-A.; Faoro, M.; Machida, A.; Mufti, A.A.; Neale, K.W.; Tadros, G. Canadian bridge design code provisions for fiber-reinforced structures. *J. Compos. Constr.* **2000**, *4*, 3–15. [CrossRef]
106. BC Ministry of Transportation and Infrastructure. *Volume 1-Supplement to CHBDC S6-14*; BC Ministry of Transportation and Infrastructure: Coquitlam, BC, Canada, 2016.
107. Allam, S.M.; Shoukry, M.S.; Rashad, G.E.; Hassan, A.S. Crack width evaluation for flexural RC members. *Alex. Eng. J.* **2012**, *51*, 211–220. [CrossRef]
108. JSCE. *Application of Continuous Fiber Reinforcing Materials to Concrete Structures*; JSCE (Japan Society of Civil Engineers): Tokyo, Japan, 1992.
109. Nanni, A. Guide for the design and construction of concrete reinforced with FRP bars (ACI 440.1 R-03). In *Structures Congress 2005: Metropolis and Beyond*; American Society of Civil Engineers (ASCE): Reston, VA, USA, 2005; pp. 1–6.
110. AASHTO-LRFD. *Bridge Design Specifications*, 2nd ed.; American Association of State Highway Transportation Officials: Washington, DC, USA, 2018.
111. El Refai, A.; Abed, F.; Al-Rahmani, A. Structural performance and serviceability of concrete beams reinforced with hybrid (GFRP and steel) bars. *Constr. Build. Mater.* **2015**, *96*, 518–529. [CrossRef]
112. Nanni, A.; De Luca, A.; Zadeh, H. *Reinforced Concrete with FRP Bars*; CRC Press: Boca Raton, FL, USA, 2014; ISBN 978-0-203-87429-5.

113. *ACI-440*; Guide for the Design and Construction of structural concrete reinforced with FRP bars (ACI 440.1 R-01). American Concrete Institute: Farmington Hills, MI, USA, 2001.
114. van Zijl, G.; Mbewe, P. Flexural modelling of steel fibre-reinforced concrete beams with and without steel bars. *Eng. Struct.* **2013**, *53*, 52–62. [CrossRef]
115. Leung, H.Y.; Balendran, R. Flexural behaviour of concrete beams internally reinforced with GFRP rods and steel rebars. *Struct. Surv.* **2003**, *21*, 146–157. [CrossRef]
116. American Concrete Institute. *Guide for the Design and Construction of Structural Concrete Reinforced with FRP Bars. 440.1 R-06*; American Concrete Institute: Farmington Hills, MI, USA, 2006.
117. CNR-DT. *Guide for the Design and Construction of Concrete Structures Reinforced with Fiber-Reinforced Polymer Bars*; National Research Council: Rome, Italy, 2006; Volume 203.
118. Rizkalla, S.H.; Aftab, A.M.; ISIS. *Reinforcing Concrete Structures with Fibre Reinforced Polymers*; ISIS Canada Research Network: Winnipeg, MB, Canada, 2001.
119. JSCE. *Recommendations for Design and Construction of Concrete Structures Using Continuous Fibre Reinforced Materials*; Japan Society of Civil Engineers: Tokyo, Japan, 1997; Volume 23.
120. Arabzadeh, A.; Rahaie, A.; Aghayari, R. A Simple Strut-and-Tie Model for Prediction of Ultimate Shear Strength of RC Deep Beams. *Int. J. Civ. Eng.* **2009**, *7*, 141–153.
121. Rasheed, M.M. Modified Softened Strut and Tie Model for Concrete Deep Beams. *J. Eng. Sustain. Dev.* **2012**, *16*, 348–361.
122. Nehdi, M.; El Chabib, H.; Saïd, A.A. Proposed shear design equations for FRP-reinforced concrete beams based on genetic algorithms approach. *J. Mater. Civ. Eng.* **2007**, *19*, 1033–1042. [CrossRef]
123. Vo-Le, D.; Tran, D.T.; Pham, T.M.; Ho-Huu, C.; Nguyen-Minh, L. Re-evaluation of shear contribution of CFRP and GFRP sheets in concrete beams post-tensioned with unbonded tendons. *Eng. Struct.* **2022**, *259*, 114173. [CrossRef]
124. Campana, S.; Fernández Ruiz, M.; Anastasi, A.; Muttoni, A. Analysis of shear-transfer actions on one-way RC members based on measured cracking pattern and failure kinematics. *Mag. Concr. Res.* **2013**, *65*, 386–404. [CrossRef]
125. Zilch, K.; Niedermeier, R.; Finckh, W. *Strengthening of Concrete Structures with ADHESIVELY Bonded Reinforcement: Design and Dimensioning of CFRP Laminates and Steel Plates*; John Wiley & Sons: Hoboken, NJ, USA, 2014.
126. Ayoubinejad, J.; Marashi, M. Investigation of fatigue phenomena and stress variations by using FRP dowel bars. *J. Struct. Constr. Eng.* **2022**, *8*, 144–155.
127. Szczech, D.; Kotynia, R. Effect of shear reinforcement ratio on the shear capacity of GFRP reinforced concrete beams. *Arch. Civ. Eng.* **2021**, *67*, 425–437.
128. Shehata, E.F. *Fibre-Reinforced Polymer (FRP) for Shear Reinforcement in Concrete Structures*; University of Manitoba: Winnipeg, MB, Canada, 1999.
129. Nasrollahzadeh, K.; Aghamohammadi, R. Reliability analysis of shear strength provisions for FRP-reinforced concrete beams. *Eng. Struct.* **2018**, *176*, 785–800. [CrossRef]
130. Choi, K.-K.; Hong-Gun, P.; Wight, J.K. Unified shear strength model for reinforced concrete beams-Part I: Development. *ACI Struct. J.* **2007**, *104*, 142.
131. Oller, E.; Marí, A.; Bairán, J.M.; Cladera, A. Shear design of reinforced concrete beams with FRP longitudinal and transverse reinforcement. *Compos. Part B Eng.* **2015**, *74*, 104–122. [CrossRef]
132. Pilakoutas, K.; Guadagnini, M. Shear of FRP RC: A review of the state-of-the-art. In *Composites in Construction: A Reality*; American Society of Civil Engineers: Capri, Italy, 2001; pp. 173–182.
133. IStructE. *Interim Guidance on the Design of Reinforced Concrete Structures Using Fibre Composite Reinforcement*; Institution of Structural Engineers: London, UK, 1999.
134. CSA. *Design of Concrete Structures*; CSA: Toronto, ON, Canada, 2004; Volume A23.
135. Taerwe, L.; Matthys, S.; Pilakoutas, K.; Guadagnini, M. *European Activities on the Use of FRP Reinforcement*; Thomas Telford Publishing: Cambridge, UK, 2001; Volume 1, pp. 3–15.
136. ICS. *Eurocode 2: Design of Concrete Structures: Part 1-1: General Rules and Rules for Buildings*; National Standards Authority of Ireland: Dublin, Ireland, 2004.
137. BSI. *Structural Use of Concrete—Design and Construction*; 8110-1; BSI: London, UK, 1997.
138. American Concrete Institute. *Building Code Requirements for Structural Concrete (ACI 318-05) and Commentary (ACI 318R-05)*; American Concrete Institute: Farmington Hills, MI, USA, 2005.
139. Lie, T.; Kodur, V. Fire resistance of steel columns filled with bar-reinforced concrete. *J. Struct. Eng.* **1996**, *122*, 30–36. [CrossRef]
140. Le, Q.X.; Dao, V.T.; Torero, J.L.; Maluk, C.; Bisby, L. Effects of temperature and temperature gradient on concrete performance at elevated temperatures. *Adv. Struct. Eng.* **2018**, *21*, 1223–1233. [CrossRef]
141. de Oliveira, A.M.; Oliveira, A.P.; Vieira, J.D.; Junior, A.N.; Cascudo, O. Study of the development of hydration of ternary cement pastes using X-ray computed microtomography, XRD-Rietveld method, TG/DTG, DSC, calorimetry and FTIR techniques. *J. Build. Eng.* **2022**, *64*, 105616. [CrossRef]
142. Naus, D.J. *The Effect of Elevated Temperature on Concrete Materials and Structures—A Literature Review*; Oak Ridge National Laboratory: Oak Ridge, TN, USA, 2006.
143. Bilow, D.N.; Kamara, M.E. Fire and Concrete Structures. In *Structures Congress 2008: Crossing Borders*; American Society of Civil Engineers: Vancouver, BC, Canada, 2008; pp. 1–10.

144. Jiang, J.; Qi, H.; Lu, Y.; Li, G.-Q.; Chen, W.; Ye, J. A state-of-the-art review on tensile membrane action in reinforced concrete floors exposed to fire. *J. Build. Eng.* **2022**, *45*, 103502. [CrossRef]
145. Buchanan, A.H.; Abu, A.K. *Structural Design for Fire Safety*; John Wiley & Sons: Hoboken, NJ, USA, 2017.
146. Hajiloo, H.; Green, M.F.; Noël, M.; Bénichou, N.; Sultan, M. GFRP-Reinforced Concrete Slabs: Fire Resistance and Design Efficiency. *J. Compos. Constr.* **2019**, *23*, 04019009. [CrossRef]
147. ASTM International Standards Organization. *Standard Test Methods for Fire Tests of Building Construction and Materials*; ASTM International Standards Organization: West Conshohocken, PA, USA, 2012.
148. Weber, A.; Witt, C.; Nadjai, A. Composite rebars in RC members in case of fire. In *Proc., Advanced Composite Materials in Bridges and Structures*; Canadian Society of Civil Engineering: Winnipeg, MB, Canada, 2008.
149. Karakurt, C. Properties of reinforced concrete steel rebars exposed to high temperatures. *Adv. Mater. Sci. Eng.* **2008**, *2008*, 814137.
150. Raj, H.; Saraf, A.; Sangal, S.; Misra, S. Residual properties of TMT steel bars after exposure to elevated temperatures. *J. Mater. Civ. Eng.* **2016**, *28*, 04015098. [CrossRef]
151. Kodur, V.; ASCE, M.; Bisby, L. Evaluation of Fire Endurance of Concrete Slabs Reinforcedwith Fiber-Reinforced Polymer Bars. *J. Struct. Eng.* **2005**, *131*, 34–43. [CrossRef]
152. Robert, M.; Benmokrane, B. Behavior of GFRP reinforcing bars subjected to extreme temperatures. *J. Compos. Constr.* **2010**, *14*, 353–360. [CrossRef]
153. Li, C.; Xian, G. Experimental and modeling study of the evolution of mechanical properties of PAN-based carbon fibers at elevated temperatures. *Materials* **2019**, *12*, 724. [CrossRef] [PubMed]
154. Feng, G.; Zhu, D.; Guo, S.; Rahman, M.Z.; Jin, Z.; Shi, C. A review on mechanical properties and deterioration mechanisms of FRP bars under severe environmental and loading conditions. *Cem. Concr. Compos.* **2022**, *134*, 104758. [CrossRef]
155. Khaneghahi, M.H.; Najafabadi, E.P.; Shoaei, P.; Oskouei, A.V. Effect of intumescent paint coating on mechanical properties of FRP bars at elevated temperature. *Polym. Test.* **2018**, *71*, 72–86. [CrossRef]
156. Benson, C.M.; Elsmore, S. Reducing fire risk in buildings: The role of fire safety expertise and governance in building and planning approval. *J. Hous. Built Environ.* **2022**, *37*, 927–950. [CrossRef]
157. Saafi, M. Effect of fire on FRP reinforced concrete members. *Compos. Struct.* **2002**, *58*, 11–20. [CrossRef]
158. Abbasi, A.; Hogg, P.J. *Fire Testing of Concrete Beams with Fibre Reinforced Plastic Rebar*; Elsevier: Amsterdam, The Netherlands, 2004; pp. 445–456.
159. Nadjai, A.; Talamona, D.; Ali, F. Fire performance of concrete beams reinforced with FRP bars. *Proc. Int. Sympsium Bond Behav. FRP Struct.* **2005**, 401–410. [CrossRef]
160. Sadek, A.W.; El-Hawary, M.; El-Deeb, A.S. Fire resistance testing of concrete beams reinforced by GFRP rebars. *J. Appl. Fire Sci.* **2006**, *14*, 91. [CrossRef]
161. Rafi, M.; Nadjai, A.; Ali, F.; O'Hare, P. Evaluation of thermal resistance of FRP reinforced concrete beams in fire. *J. Struct. Fire Eng.* **2011**, *2*, 91–107. [CrossRef]
162. Lin, X.; Zhang, Y. Nonlinear finite element analyses of steel/FRP-reinforced concrete beams in fire conditions. *Compos. Struct.* **2013**, *97*, 277–285. [CrossRef]
163. Hawileh, R.; Naser, M. Thermal-stress analysis of RC beams reinforced with GFRP bars. *Compos. Part B Eng.* **2012**, *43*, 2135–2142. [CrossRef]
164. Carvelli, V.; Pisani, M.A.; Poggi, C. High temperature effects on concrete members reinforced with GFRP rebars. *Compos. Part B Eng.* **2013**, *54*, 125–132. [CrossRef]

Disclaimer/Publisher's Note: The statements, opinions and data contained in all publications are solely those of the individual author(s) and contributor(s) and not of MDPI and/or the editor(s). MDPI and/or the editor(s) disclaim responsibility for any injury to people or property resulting from any ideas, methods, instructions or products referred to in the content.